Proceedings of the 11th World Congress on Mechanical, Chemical, and Material Engineering (MCM'25)
Paris, France - August, 2025
Paper No. ICMIE 178
DOI: 10.11159/icmie25.178

A Finite Element Approach to Optimize Fiber Paths of Tow Steered Composites Using Unstructured Mesh Technique

Altan Kayran[1], Rameezul Haq[2]
Department of Aerospace Engineering, Middle East Technical University
Üniversiteler Mahallesi, Dumlupınar Bulvarı No:1 06800, Çankaya Ankara, Türkiye
[1]akayran@metu.edu.tr; [2]rameezul.haq@metu.edu.tr

***Abstract* -** This study proposes a finite element-based methodology to optimize curvilinear fiber paths in Tow Steered Composites (TSCs) by tuning two governing fiber orientation parameters, T_0 and T_1. These angles define the spatially varying fiber direction along the lamina, directly influencing structural stiffness and buckling behaviour. MATLAB is employed to extract the complete central fiber path definitions for a flat square plate made up of a single lamina, with parametric sweep of 81 combinations of (T_0, T_1), the sole parameters which govern the central fiber path. For the purpose of finite element modelling, a novel approach of executing unstructured mesh is adopted in ANSYS Workbench, with an objective to cover the no overlap and overlap regions precisely for each of the combinations of (T_0, T_1) in the entire plate, subsequently the combinations are evaluated by first conducting simple static structural analysis under axial compression, followed by linear eigenvalue buckling analysis. Buckling load factors are extracted to identify optimal fiber path configurations. While overlap-related defects from fiber placement are acknowledged, the shift distance optimization is discussed as future work. The findings highlight the critical role of fiber orientation tailoring in maximizing structural performance under compressive loads.

***Keywords*:** Optimization, Tow Steered Composites, Finite Element, Buckling Load Factor, Unstructured Mesh, Overlaps

1. Introduction

Tow Steered Composites (TSCs) are an advanced class of fiber-reinforced materials where the fiber paths are not restricted to straight lines but can follow curvilinear trajectories across the laminate surface. This ability to steer fibers introduces variable stiffness in the structure, which can be exploited to tailor load paths, enhance local stiffness, and improve overall structural efficiency [1]. In aerospace and high-performance structural applications, where buckling, strength-to-weight ratio and aeroelastic performance are primary concerns, such design flexibility is invaluable. Unlike traditional composite laminates, where stiffness is uniform and constrained by straight-fiber alignment, TSCs enable the development of components that are optimized to redirect load paths, resist local stress concentrations, and delay the onset of buckling [2]. However, the practical performance benefits of TSCs rely not only on the ability to steer fibers, but more critically on how the fiber paths are parametrically defined and strategically optimized. Manufacturing constraints such as tow width, tow path curvature limits, and the possibility of overlaps or gaps must be considered alongside structural performance metrics [3]. Additionally, due to the curvilinear nature of the fibers, analytical modelling becomes challenging, and finite element analysis is often essential to evaluate the real structural response under load. Designing efficient TSCs therefore becomes a multi-disciplinary challenge involving geometry, mechanics, and manufacturability.

Multiple methodologies have been developed in literature for the modelling of curvilinear fiber tows under the finite element domain. Blom et al. [4] modelled the curvilinear tows and defects (gaps/overlaps) using structured mesh for a flat simply supported plate, such that the elements were either filled with composite material or resin only (gaps). This implies that the elements comprising of both, regular thickness tow and gaps/overlaps, would be simplified to either be of regular thickness or gaps/overlaps. Fayazbakhsh et al. [5] utilized a modified methodology of defect layer to model and capture the effect of gaps and overlaps in variable stiffness laminates, where again a structured mesh over the plate was laid down. Brampton et al. [6] designed a new approach 'level set method' for TSC optimization, where no gaps and overlaps were considered and again a structured mesh was exercised.

This study focuses specifically on optimizing the central fiber path of a TSC laminate using two governing angular parameters: T_0 and T_1, which dictate the orientation at different regions across the panel width [7]. These angles define the fiber orientation at key positions along the x-axis of the plate, namely at the edges (T_0) and quarter-span regions (T_1). This formulation enables the generation of symmetric, curvilinear fiber paths across the plate. The rationale for selecting only two parameters lies in the balance between design simplicity and effective stiffness tailoring. A novel approach of laying down unstructured mesh is implemented on a flat plate of 30 cm by 30 cm dimensions, such that no over simplification is made and the defect regions (only overlaps in this study) are precisely and accurately covered over the lamina. An automatic fiber placement (AFP) machine capable of placing a single course consisting of 3 tows, each of 0.3175 cm of width [8], is assumed to be employed for this particular use-case of ours. For simplicity, the total course width of 0.9525 cm is rounded off to a constant width of 1 cm for our application. The central course is then shifted along the y axis by a minimum value such that the entire plate is covered. By systematically evaluating different combinations of T_0 and T_1, this work aims to identify the fiber path configuration that maximizes the buckling load factor, serving as a key performance indicator for the laminate's structural stability.

2. Fiber Path Modelling and Parametric Setup

2.1. Geometric Representation

The central fiber path is defined on a square lamina of side length 'a'. The orientation angle along the x-axis varies according to a piecewise-symmetric pattern: T(x=−a) = T_0, T(x=−a/2) = T_1, T(x=0) = T_0, T(x=a/2) = T_1, and T(x=a) = T_0. Figure 1 below depicts the reference fiber path and corresponding fiber orientation for a <0|50> fiber lamina, chosen arbitrarily as a base combination for explanatory purposes, where <0|50> refers to $<T_0|T_1>$ which is the general nomenclature used to define the central fiber path for a TSC.

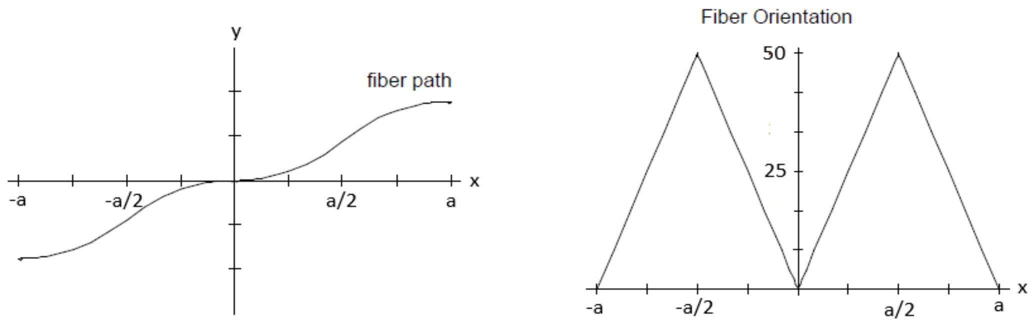

Fig. 1: <0|50> central fiber path and orientation.

This arrangement of orientation angle variation piecewise ensures geometric symmetry about the laminate centerline, which is essential for consistent load transfer and structural response under axial loading. Importantly, the fiber orientation is independent of the y-coordinate, making this a 1-dimensional steering formulation in the x-direction.

Given known expressions for θ(x) and y(x), the full spatial profile of the central fiber is reconstructed. The equations were extracted from [9] which provides the relationships between θ and x, and y and x. A course of 1 cm of constant width and thickness of 1mm is assumed to be placed over this trajectory.

2.2. Design of Experiments

To explore design space, a full factorial combination of T_0, $T_1 \in \{0^\circ, 10^\circ, 20^\circ \ldots, 80^\circ\}$ is generated, with an interval of 10°, yielding 81 configurations. This systematic sweep ensures coverage from straight to highly curved fiber paths.

Each configuration produces a distinct central course shape and, by vertical shifting, a complete lamina without any fiber gaps. The minimum shift distances (i.e. the minimum absolute difference in y at each instance of x for a tow) required to evade gaps defects are first calculated through a MATLAB script, and subsequently utilized to construct the complete lamina. The rationale for using the minimum shift distance lies in the manufacturing robustness it offers. Overlaps, while suboptimal, do not leave regions unreinforced. This conservative assumption ensures load continuity and avoids sharp discontinuities associated with gaps, which can serve as failure initiation sites. While overlaps are present, this conservative choice prevents reinforcement voids—critical in preventing local failures. The following Table 1 tabulates the minimum shift distances for each of the combinations. Note how the diagonal cells in the table below are left empty where $T_0 = T_1$, since no shift distance and thereby no overlaps exist for these cases as the fibers would be of straight paths.

Table 1: Minimum shift distances (cm) for various combinations of (T_0, T_1).

	T_0								
T_1	0°	10°	20°	30°	40°	50°	60°	70°	80°
0°		1.000	1.000	1.000	1.000	1.000	1.000	1.000	1.000
10°	1.000		1.016	1.016	1.016	1.016	1.016	1.017	1.017
20°	1.000	1.016		1.065	1.066	1.067	1.067	1.068	1.069
30°	1.000	1.016	1.065		1.157	1.159	1.161	1.163	1.165
40°	1.000	1.016	1.065	1.156		1.310	1.314	1.318	1.323
50°	1.000	1.016	1.065	1.157	1.308		1.564	1.573	1.582
60°	1.000	1.016	1.066	1.158	1.310	1.560		2.018	2.036
70°	1.000	1.016	1.066	1.159	1.312	1.564	2.009		2.969
80°	1.000	1.016	1.067	1.160	1.314	1.569	2.018	2.947	

A square plate of dimensions of 30 cm by 30 cm is taken as a sample size of the lamina, and a constant course width methodology was used for the construction of the composite lamina through shifting, instead of the constant vertical distance methodology [5]. The latter comes at a cost of added mechanical complexity, higher investment, maintenance and operational expenses for AFP machines, whereas a relatively simpler approach would be to, instead, keep the course width constant with no additionally attached tow-drop mechanism in the machine. This essentially renders the application to shapes, such as flat panels or parts with simple curves, fairly straight forward. Figure 2 below illustrates the complete composite single layer lamina constructed in MATLAB by using the minimum shift distance defined for the <0|50> fiber path, where a regions of single thickness is shown in light-blue and regions of tow overlaps are marked in dark-blue.

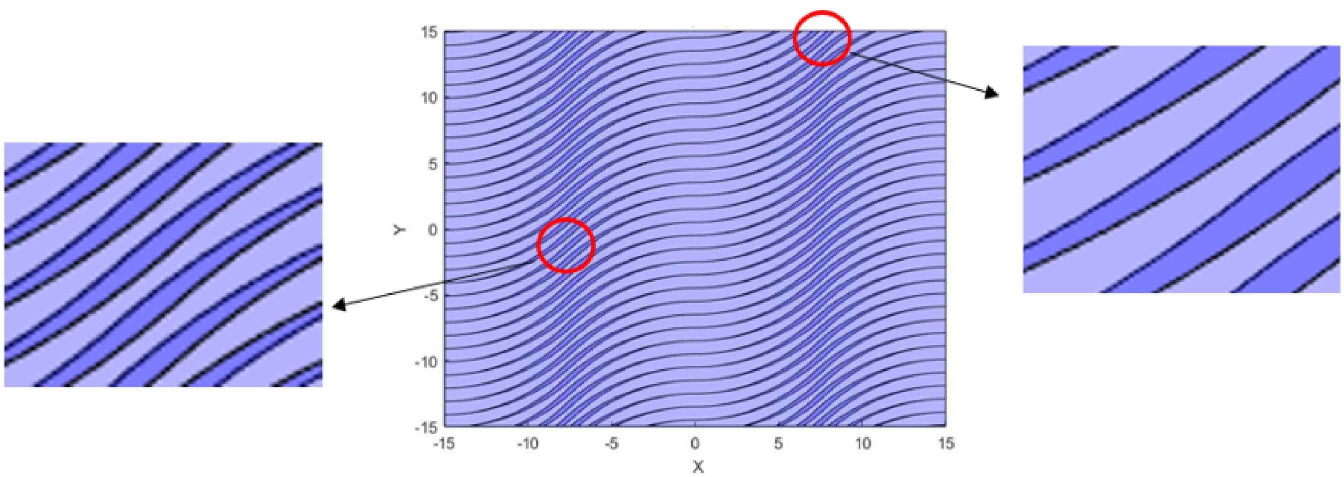

Fig. 2: Lamina defined by <0|50> fiber path

An additional script was developed in MATLAB to calculate the total sum of overlap areas (cm^2) for each of the combinations of (T_0, T_1) mathematically, and is presented in the form of a table in Table 2 below.

Table 2: Total overlap area (cm^2) for various combinations of (T_0, T_1).

	T_0								
T_1	0°	10°	20°	30°	40°	50°	60°	70°	80°
0°		164.635	175.743	197.303	229.018	276.938	350.240	429.473	489.055
10°	163.808		176.068	200.660	237.218	290.785	371.060	459.098	522.740
20°	176.213	175.935		188.603	228.815	286.660	372.670	475.448	546.273
30°	196.020	200.403	188.523		203.488	263.948	353.743	476.353	560.518
40°	226.568	236.623	228.675	203.595		222.458	313.428	455.688	564.920
50°	275.213	289.403	286.058	264.273	222.933		250.125	395.663	557.408
60°	345.445	368.765	371.410	353.653	314.383	251.395		298.868	527.408
70°	426.225	456.348	473.470	475.738	456.918	397.828	301.005		419.423
80°	484.240	518.195	542.455	557.938	563.950	558.108	530.103	423.693	

3. Finite Element Analysis for Buckling Evaluation

3.1. Simulation Setup

Each lamina is modelled using Quad-Dominant shell elements in ANSYS, reflecting the slenderness of composite panels and their dominance of bending-driven failure modes. Course/tow is assigned 1 mm of shell thickness. Linear elemental order is used for the shell elements, with `SHELL181` adopted as the default shell element type. Although the geometry is a single shell body, face cuts were made onto the body to distinguish between single thicknesses regions and overlap regions. A general mesh element size of 1 mm is carefully chosen, such that the overlaps regions are precisely captured. Because the faces of single thickness regions and overlap regions were now distinct, this resulted in the generation of an unstructured mesh over the complete body. Note that the total number of mesh elements were not constant and varied across all of the combinations, since the mesh is generated separately one by one for each unique combination of (T_0, T_1). For the base case of <0|50>, Figure 3a below illustrates the modelling of geometry without and Figure 3b with the face cuts, while Figure 4a displays the thickness distribution over the lamina modelled as a shell body and Figure 4b shows the central fiber path (given as an input to define general fiber direction) in ANSYS ACP Pre.

Fig. 3a: Shell body with no face cuts

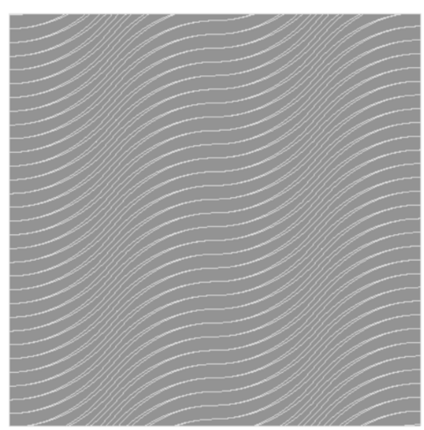

Fig. 3b: Shell body with face cuts

Figure 3: Shell body with and without face cuts

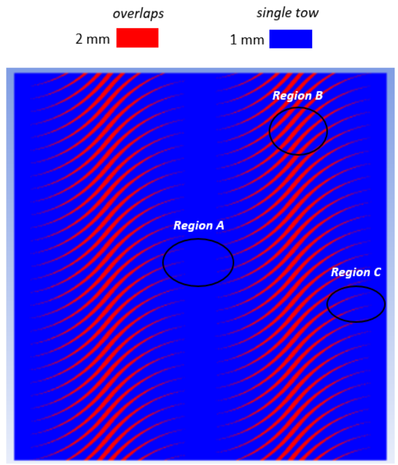

Fig. 4a: Thickness distribution

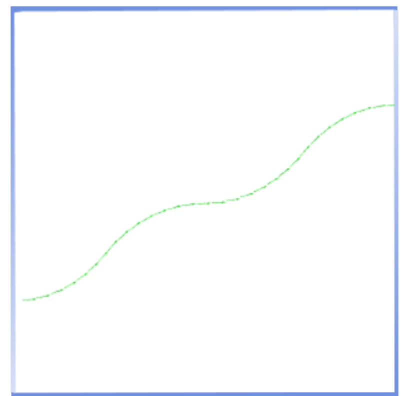

Fig. 4b: Central fiber path

Figure 4: Thickness distribution and Central fiber path

Figure 5a beneath shows the structured mesh over the shell body if no face cuts were to be implemented, and Figures 5b, 5c and 5d demonstrates the mesh constructed using unstructured meshing with the face cuts at the regions A, B and C, in Fig. 4a, respectively. The latter technique holds the ability to properly capture all the intricacies existing due to the region of overlaps.

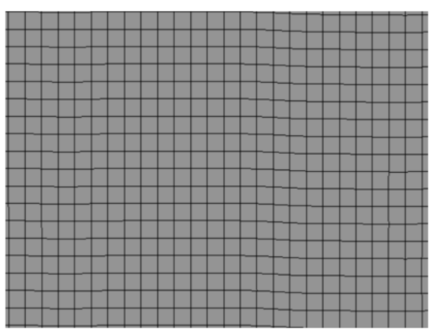

Fig. 5a: Structured mesh

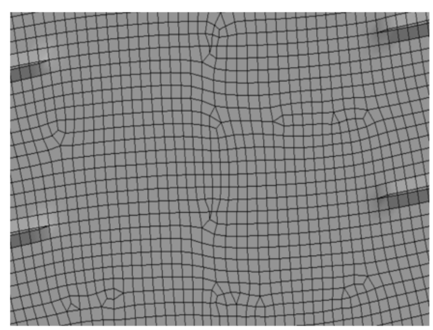

Fig. 5b: Unstructured mesh (Region A)

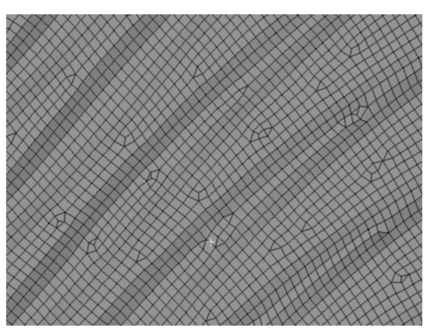

Fig. 5c: Unstructured mesh (Region B)

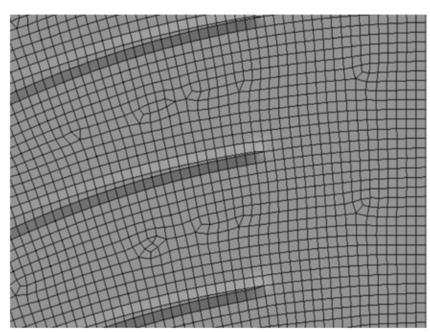

Fig. 5d: Unstructured mesh (Region C)

Fig. 5: Structured and Unstructured mesh

Initially, a static structural analysis was conducted for all shell body for 81 combinations of (T_0, T_1), followed by an eigenvalue linear buckling analysis for each. The ANSYS Workbench was linked to MATLAB such that the overall process of first generating the data for central fiber path in MATLAB for each configuration would be imported automatically to ANSYS, where it carries out the actions of central course construction, shifting of central course vertically by the minimum shift distance to cover the entire body, face cuts, mesh generation, thickness allocations in ACP Pre, conducting static structural and subsequently eigenvalue linear buckling analysis, one by one for all the combinations in an automated fashion. A unit axial compressive load was applied to the body, and simply supported boundary conditions were ideally chosen such that it suppresses rigid body motion without over-constraining deformation, as depicted in Figure 6.

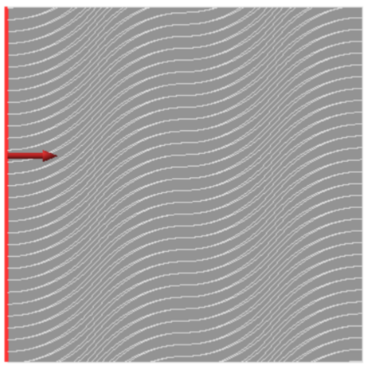

Fig. 6a: Unit load applied on left edge

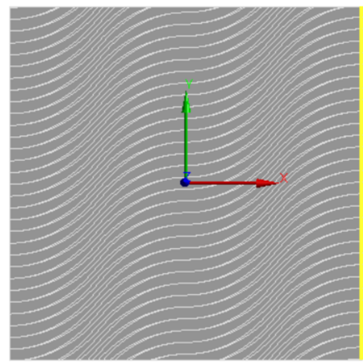

Fig. 6b: T_y= T_z=R_x=R_y=R_z= free, T_x= 0

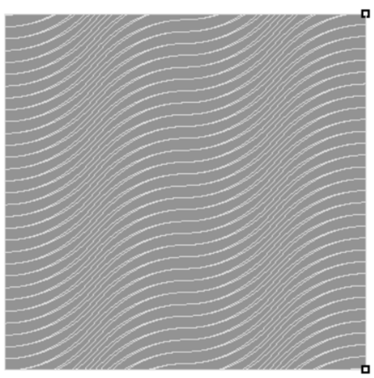

Fig. 6c: T_x= T_z=R_x=R_y=R_z= free, T_y= 0

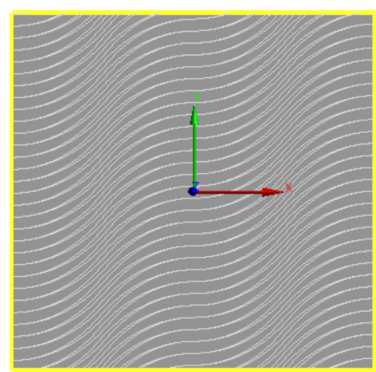

Fig. 6d: T_x= T_y=R_x=R_y=R_z= free, T_z= 0

Fig. 6: Load application and Boundary conditions ($T_{x,y,z}$ = translations, $R_{x,y,z}$ = rotations)

3.2. Buckling Load Factor as a Performance Metric

The buckling load factor (BLF) is extracted from a linear buckling analysis. This metric reflects the amplification of the applied load required to initiate instability. The fiber path influences the BLF through three coupled effects:

1. ***Stiffness Distribution***: The local stiffness of a lamina shell varies with fiber orientation. Configurations where fibers align more closely with the compressive load direction exhibit enhanced axial stiffness, thus raising the buckling threshold.
2. ***Load Path Steering***: Curvilinear fibers can redistribute loads across the panel, minimizing localized instabilities and promoting global buckling modes over local ones.
3. ***Tow Overlaps***: The extent of tow overlap, inherently resulting from the minimum shift distance approach, also plays a subtle but important role. While overlaps are often considered manufacturing imperfections, they increase local thickness and stiffness in regions where multiple tows converge. This local reinforcement effect can elevate the panel’s buckling capacity, especially when overlaps align favourably with compressive load paths. However, excessive or randomly

distributed overlaps may induce stiffness discontinuities, potentially affecting post-buckling behaviour — a trade-off that will be addressed in future shift distance optimization studies.

A table is constructed which features the BLF values obtained from buckling analysis for each of the combinations, as displayed in Table 3. Note how the diagonal elements in the table are entered in the *Italic* format to distinguish them from the rest of the elements, since they represent the cases where the lamina itself solely constitutes of straight fibers, with no overlap regions. For these particular cases, it is evident from the table how the BLF keeps on dropping as we proceed from 0°(greatest fiber alignment with load direction) to 80°(least fiber alignment with load direction) since thickness buildup due to overlaps does not play a part here in BLF computations.

Table 3: BLF values for various combinations of (T_0, T_1).

	T_0								
T_1	0°	10°	20°	30°	40°	50°	60°	70°	80°
0°	*481.69*	485.43	540.71	608.46	695.55	814.33	1004.95	1645.47	3158.48
10°	486.76	*470.79*	527.18	612.17	692.95	801.18	1020.38	1699.11	3244.07
20°	541.19	525.86	*439.94*	536.01	619.57	730.54	956.66	1601.89	2960.81
30°	602.55	597.08	522.68	*403.98*	519.62	640.83	855.63	1373.99	2369.25
40°	669.86	668.51	607.06	507.53	*378.19*	530.89	726.57	1029.45	1986.62
50°	757.28	761.35	707.47	620.21	509.44	*362.20*	524.69	723.58	1453.97
60°	935.99	960.17	909.17	812.44	686.08	536.04	*344.05*	505.63	982.78
70°	1770.22	1592.19	1537.64	1365.78	1083.76	789.13	574.43	*294.61*	511.59
80°	3650.83	3627.88	3357.91	2853.72	2270.17	1706.5	1153.47	692.66	*260.59*

Through analysing the current table, the configuration with the maximum BLF is identified as the optimal fiber path. This result directly correlates with superior structural performance under compressive loads. Figure 7 demonstrates the first buckling mode and the corresponding BLF for the lamina defined by <0|80> fiber path (BLF = 3650.83), since it gives the maximum BLF.

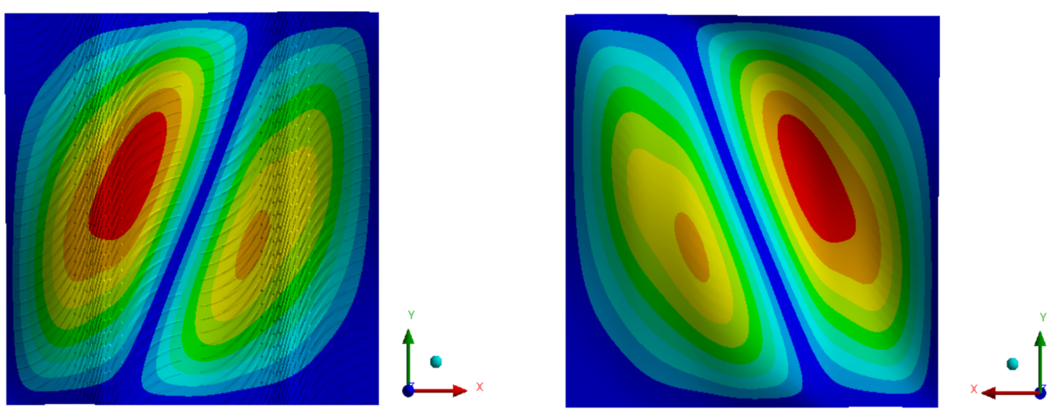

Fig. 7: First buckling mode shape with BLF = 3650.83 for optimal configuration of <0|80>

4. Discussion on Placement Effects and Future Optimization

While this study prioritizes fiber path optimization, the influence of tow shifting strategy is also acknowledged. The choice of minimum shift distance ensures uninterrupted fiber coverage and manufacturing feasibility. Overlaps, although potential defect sources, are more acceptable than gaps, which can lead to significant local stress concentrations and premature failure [10].

However, in practice, a balance must be struck between manufacturability and structural performance. Future work will introduce an optimization routine—employing Genetic Algorithms and FMINCON—to fine-tune shift distances. A minimum shift distance corresponds to an all overlap case (with no gaps), while a maximum shift distance proposes an all gap case (with no overlap). The intended optimization will aim acquire a ideal shift distance lying between the two, to minimize the combined area of overlaps and gaps, while considering BLF, mass, and Tsai-Hill failure criteria in a unified performance index.

5. Conclusion

This work presents a robust finite element-based framework for optimizing fiber paths in Tow Steered Composites using a novel approach of utilizing the unstructured meshing technique in ANSYS Workbench. By parametrizing the path with just two angles, T_0 and T_1, and evaluating the structural response via the buckling load factors, the method identifies configurations that significantly enhance load-bearing performance. It is discovered that the neither those combinations which align most closely to the load direction (such as <0|10>, <10|0>, etc) nor the combinations which results in the most amount of overlaps area (such as <40|80>, <80|40>, etc) comes out as the one with the maximum BLF; instead an in-between fiber path defined by <0|80> produces the highest BLF, which indicates why a proper optimization methodology should be executed to gain high structural performance and efficiency.

While the shift distance for lamina construction is treated conservatively here, future refinements will target manufacturability-performance trade-offs. Overall, this approach contributes toward practical design strategies for next-generation variable stiffness composite structures.

Acknowledgement

The support provided by the Scientific and Technological Research Council of Türkiye (TÜBİTAK) through the '2224-A Grant Program for Participation in Scientific Meetings Abroad' is gratefully acknowledged.

References

[1] R. A. Olmedo, “Compression and Buckling of Composite Panels with Curvilinear Fibers,” M.S. dissertation, Dept. Eng. Mechs., Virginia Polytechnic Institute and State Univ., Blacksburg, VA, 1992.

[2] A. A. Vijayachandran and A. M. Waas, “Minimizing stress concentrations using steered fiberpaths and incorporating realistic manufacturing signatures,” *International Journal of Non-Linear Mechanics*, vol. 146, no. 3, 2022.

[3] T. R. Brooks and J. Martin, “On manufacturing constraints for tow-steered composite design optimization,” *Composite Structures*, vol. 204, pp. 548-559, 2018.

[4] A. W. Blom, C.S. Lopes, P. J. Kromijk, Z. Gurdal and P. P. Camanho, “A Theoretical Model to Study the Influence of Tow-drop Areas on the Stiffness and Strength of Variable-stiffness Laminates,” *Journal of Composite Materials*, vol. 43, no. 5, pp. 403-425, 2009.

[5] K. Fayazbakhsh, M. A. Nik, D. Pasini and L. Lessard, “Defect layer method to capture effect of gaps and overlaps in variable stiffness laminates made by Automated Fiber Placement,” *Composite Structures*, vol. 97, pp. 245-251, 2013.

[6] C. J. Brampton, K. C. Wu and H. A. Kim, “New optimization method for steered fiber composites using the level set method,” *Structural and Multidisciplinary Optimization*, vol. 52, pp. 493–505, 2015.

[7] Z. Gurdal and R. Olmedo, “In-Plane Response of Laminates with Spatially Varying Fiber Orientations: Variable Stiffness Concept,” *AIAA Journal*, vol. 31, no. 4, pp. 751-758, 1993.

[8] K. C. Wu, “Design and analysis of tow-steered composite shells using fiber placement,” in *American society for composites 23rd annual technical conference*, Memphis, TN, 2008.

[9] C. Waldhart, “Analysis of Tow-Placed, Variable-Stiffness Laminates,” M.S. dissertation, Dept. Eng. Mechs., Virginia Polytechnic Institute and State Univ., Blacksburg, VA, 1996.

[10] Z. Gurdal and B. F. Tatting, “Tow-Placement Technology and Fabrication Issues for Laminated Composite Structures,” in *46th AIAA/ASME/AHS/ASC structures, structural dynamics and materials conference*, Austin, TX, 2005.